

Estimation of Surface Temperature and Heat Flux over a Hollow Cylinder and Slab using an Inverse Heat Conduction Approach

Apoorva Deep Roy – Sushil Kumar Dhiman*

Department of Mechanical Engineering, Birla Institute of Technology, India

A non-iterative approximation of the inverse heat conduction problem has been developed through energy balance between the control volumes. The heat flow domain along the surface normal was divided into three control volumes and studied in three cases, specifically on a heated hollow metallic cylinder cooled in crossflow of air, a heating flat plate in still air, and a heated flat plate when cooled in still air with random air blows. The time derivatives of temperature and heat flux estimates at the surface appearing in derived equations were evaluated by approximate expressions. Both estimates were obtained from the derived equations by simultaneous measurement of temperature-time histories at two locations: one at the inner surface and the other anywhere within the control volume along the surface normal. The deviation was checked by real-time simultaneous measurement of temperature-time history at the outer surface along the normal surface. Comparison between the estimated surface temperature-time history using the derived equations and the real-time measurement showed deviations within 0.5 % for the cylinder, within 0.03 % for the plate in still air and within 0.5 % when air blows were given. Heat fluxes estimated using these time histories were correspondingly arrived at consistent and close approximations for all cases. Estimates from the derived equations were compared with reported equations from the literature, and a wind tunnel experiment for the validation of circumferential distribution of heat transfer was conducted, for which they also showed reasonably good agreements.

Keywords: surface temperature and heat flux, inverse heat conduction, energy balance approach, hollow cylinder and flat plate, derived equations

Highlights

- A non-iterative approximation of the inverse heat conduction problem has been developed through energy balance between the control volumes.
- Three cases were studied: on a heated hollow metallic cylinder cooled in crossflow of air, a heating flat plate in still air, and a heated flat plate when cooled in still air with random air blows.
- Estimates of surface temperature and heat flux were obtained by derived equations.
- The developed methodology was tested experimentally and validated from the reported literature.

0 INTRODUCTION

In many engineering applications, such as rocket nozzles, boiler tubes, nuclear reactors, etc., where high temperatures and pressures persist, a direct measurement of surface temperature and heat flux may lead to the burning of sensors as well as create disturbances in fluid flow structures. To handle such situations, the sensors were placed in some interior positions within the solid to capture temperature histories so that the corresponding surface temperature histories and heat flux could be estimated. Such a problem (or approach) is referred to as inverse heat conduction problem (IHCP) or inverse heat conduction approach.

Hollow cylinders have been extensively used in the aforementioned industries under various types of heat exchangers, including boiler tubes, reheater tubes, superheater tubes, etc. In engineering applications, such as rocket nozzles and hard material machining, etc., slabs are used for which IHCP's solution techniques are utilized to estimate the surface temperature and heat flux.

The solution of an IHCP is studied in domains of direct and inverse problems. The direct problem uses the known boundary conditions, and the variation within the solid is investigated. However, under an inverse problem, which is mathematically ill-posed in nature, only one boundary condition is known, and it requires some special techniques of solutions. Here, the prime importance is given to errors in measurement. The measurement error should be minimized to obtain close approximations of the estimates. Many iterative or non-iterative techniques have been presented to minimize the errors in measurements.

Taler [1] utilized a singular value decomposition method and the Levenburg-Marquardt method (LMM) to solve IHCP and reported that the singular value decomposition method takes less computational time. Golsorkhi and Tehrani [2] utilized LMM and a finite volume method (FEM); Cuadrado et al. [3] proposed a non-iterative approach, whereas Bohacek et al. [4] utilized minimizing the Least Squares norm between experimental and simulated data to obtain a solution of an IHCP.

Felde and Reti [5] presented an iterative inverse algorithm to solve IHCP for evaluation of the hardening performance of cooling media. Charifi and Zegadi [6] utilised an inverse global descent method based on a finite difference method to solve an inverse problem for spherical geometry solidification. Gostimirović et al. [7] used a numerical method with finite differences in an implicit form to predict grinding wheel and workpiece interface surface temperature as well as heat flux by measuring time temperature history at the interior surface. Hribersek et al. [8] determined the surface heat transfer coefficient for nitrogen in liquid and gaseous phases on an Inconel 718 workpiece by numerical simulation.

Stolz [9] solved an IHCP for shapes like slabs, cylinders, and spheres kept at different thermal conditions in a fluid medium by the principle of superposition. The formulation was done by measuring transient temperature in proximity to the outer surface of the solid. To obtain an IHCP solution, Frank [10] applied the least-squares method on experimentally determined temperatures. Sparrow et al. [11] presented an integral technique coupled with finite difference approximation to obtain the solution of an IHCP by the measurement of transient temperature within the solid of different shapes. Beck and Wolf [12] and Beck [13] analysed the non-linear IHCP and solved it using the finite difference method (FDM).

Imber and Khan [14] presented an approximation method for the solution of IHCP consisting of a polynomial function, and they implanted thermocouples to measure the transient temperature inside the solid. Space-marching methods have been utilized to obtain the solution of IHCP [15] and [16]. Li and Yan [17] estimated heat flux by using the conjugate gradient method. Masanori et al. [18] utilized the Laplace transform technique, considering cylindrical, spherical, and rectangular coordinates by measuring the transient temperature at two interior locations within a body for solving IHCP. Chen et al. [19] presented a solution of IHCP on a circular pipe with turbulent fluid flow by measuring the temperature within the fluid at different locations.

Jang et al. [20] formulated an IHCP solution method by using a finite-element scheme and an input estimation method on the hollow cylinders. Chen et al. [21] carried out an analysis on a circular pipe with laminar fluid flow and solved the IHCP using the matrix system form of governing equations.

Wikstrom et al. [22] estimated surface heat flux and temperature by recording transient temperatures at three different locations in a thick slab by using the Crank-Nicholson implicit scheme. Dennis and

Dulikravich [23] solved a three-dimensional IHCP by using FEM. Kim and Lee [24] suggested a maximum entropy method to get a solution for an IHCP. The space marching method has been utilized to predict the control rod stem surface temperature [25].

Dhiman and Prasad [26] used LMM coupled with Duhamel's theorem, whereas Singh et al. [27] utilised LMM coupled with truncated Fourier series for solving IHCP. Cebula et al. [28] used the finite element-finite volume method to obtain the solution of an IHCP. Duda and Konieczny [29] proposed a new method to solve IHCP for a complex configuration. Mehta [30] estimated the outer surface heat flux of a rocket nozzle by using FDM. Da Silva et al. [31] estimated the heat transfer coefficient in a stacked microchip by using fundamental solutions. Shahnazari et al. [32] and Matsevityi et al. [33] formulated a hybrid method.

Seryakov [34] presented a mathematical formulation, Gomez et al. [35] presented a virtual experiment approach, whereas Leu and Tu [36] proposed a hybrid exact solution method to solve IHCP. Cialkowski et al. [37] solved an IHCP to obtain the surface temperature on a gas turbine blade coated with ceramics. A literature review was presented by Roy and Dhiman [38] to discuss the various methods of finding solutions for IHCP.

The brief literature review presented above clearly indicates that the profound utilization of IHCP in numerous research studies has been carried out in previous decades. The technological developments in recent decades have been a result of the search for alternative possible methodologies or mathematical approaches that closely estimate the unknown parameter. Hence, there is always a scope for the development of novel mathematical approaches which, if available, can be readily utilized to accomplish the tasks. The research gap in the present approach highlights the use of the heat flow domain fragmented into several control volumes and analysis of their energy balance equations, which is a novel work in the IHCP approach.

The advantages of using the present methodology can be highlighted as an inverse approach that provides a very close-exact solution with simplicity in equations, based on a non-iterative approach of approximating the estimates and being able to treat linear inverse heat conduction problems with data containing random errors. Typically, while solving IHCPs, errors in the temperature data affect the accuracy of the difference approximation of time derivatives, which leads to large errors. The present technique does not involve sequential stepping

forward in time and overcomes the above-mentioned drawback. It is also not necessary under the presented technique to compute all the nodal temperatures at each time step. In contrast to most previous IHCP solution methods, this method does not require any information about the initial temperature distribution in the solid. The surface heat flux at a specific time can be directly calculated from the transient measured temperature inside a solid without step-by-step computation in the time domain.

The present paper aims to develop a methodology based on a non-iterative approach of approximating the estimates through IHCP. To validate the derived estimate equations, experiments are performed on a heated hollow metallic cylinder cooled in crossflow of air, a heating flat plate in still air, and a heating flat plate with random air blows when cooled in still air. The surface temperature and heat flux were estimated by acquiring time histories of temperature at some interior location of the solid by means of a T-type thermocouple in all the cases.

The estimated results were compared with the measured real-time surface temperature and calculated surface heat flux. The derived equation outcomes were also compared with the results of the exact solution from the reported literature for the flat plate.

1 PROBLEM STATEMENT AND ANALYSIS

Consider a hollow metallic cylinder initially heated with a constant heat flux condition, assuming that the entire wall of the cylinder is at a uniform temperature. Here, “initially” refers to the condition when no external flow of fluid is given across the cylinder, while the “constant heat flux” refers to the heat flux provided to the cylinder is the same all the time, i.e., initially as well as when its external surface is exposed to the fluid flow.

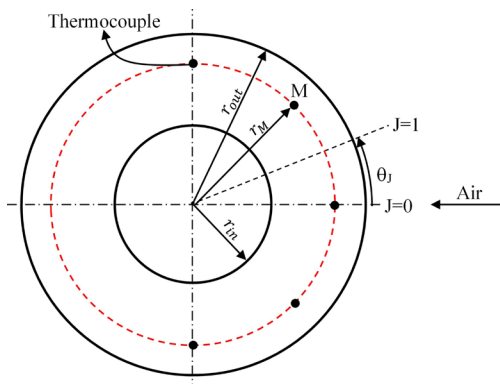


Fig. 1. Schematic view of a heated hollow cylinder in the flow of air

Referring to Fig. 1 as per the cylindrical coordinate system where a hollow cylinder has been shown with inner and outer radii r_{in} and r_{out} and an intermediate radius r_M . The region between r_{in} and r_M represents the direct region, while the region between r_M and r_{out} represents the inverse region.

Referring to Fig.2, a plan of inverse analysis in a quadrant of the cylinder is considered. Three control volumes (cv) cv_1 , cv_2 , and cv_3 , named radially inwards, have been considered in the Inverse region of step size Δr . Each of these control volumes have been provided a central node ($L=0, 1, 2, \dots, M-3, M-2, M-1, M, M+1$) by considering node $M-2$ at r_{out} (at $L=M-2=1$ if $r_{out}=r_1$), node M at r_M (or at $L=M=3$ if $r_M=r_3$), node $M-1$ at r_{M-1} (or at $L=M-1=2$ if $r_{M-1}=r_2$), node $M+1$ at r_{M+1} (or at $L=M+1=4$ if $r_{M+1}=r_4$) and node F at r_{in} . Of all these nodes, node F and node M represent the real-time measurement locations, and node $M-2$ is the real-time estimated location. To complete the solution, a fictitious node $M-3$ with step size Δr has been assumed beyond $r_{(M-2)}$.

In addition, the corresponding radii of outer control surfaces $r'_{(M-2)}$, $r'_{(M-1)}$, r'_M , and $r'_{(M+1)}$ have been considered, for instance, $r'_M=r_M+(\Delta r/2)$.

1.1 Problem Statement

A heated hollow cylinder of isotropic material having no internal heat generation, when subjected to an external flow of fluid of constant fluid properties, undergoes unsteady temperature variation at any point on its surface. Hence, a one-dimensional mathematical statement of the problem can be represented in cylindrical coordinates as [39]:

$$\frac{\partial^2 T}{\partial r^2} + \frac{1}{r} \frac{\partial T}{\partial r} = \frac{1}{\alpha} \frac{\partial T}{\partial t},$$

for $r_M \leq r \leq r_{out}$ and $t > 0$. (1)

The heat conduction in the r -direction through the direct region provides the heat flux q_M to the Inverse region, which is expressed as [39]:

$$q_M(t) = -K \left(\frac{\partial T(r,t)}{\partial r} \right) \text{ at } r = r_M,$$

for times $t = t_j, j = 1, 2, \dots, N$. (2)

We may write the Newton’s law for convective heat transfer in terms of convective coefficient as [39]:

$$h(t) = \left(\frac{q_1(t)}{T_1(t) - T_\infty} \right) \text{ at } r = r_{out},$$

for times $t = t_j, j = 1, 2, \dots, N$. (3)

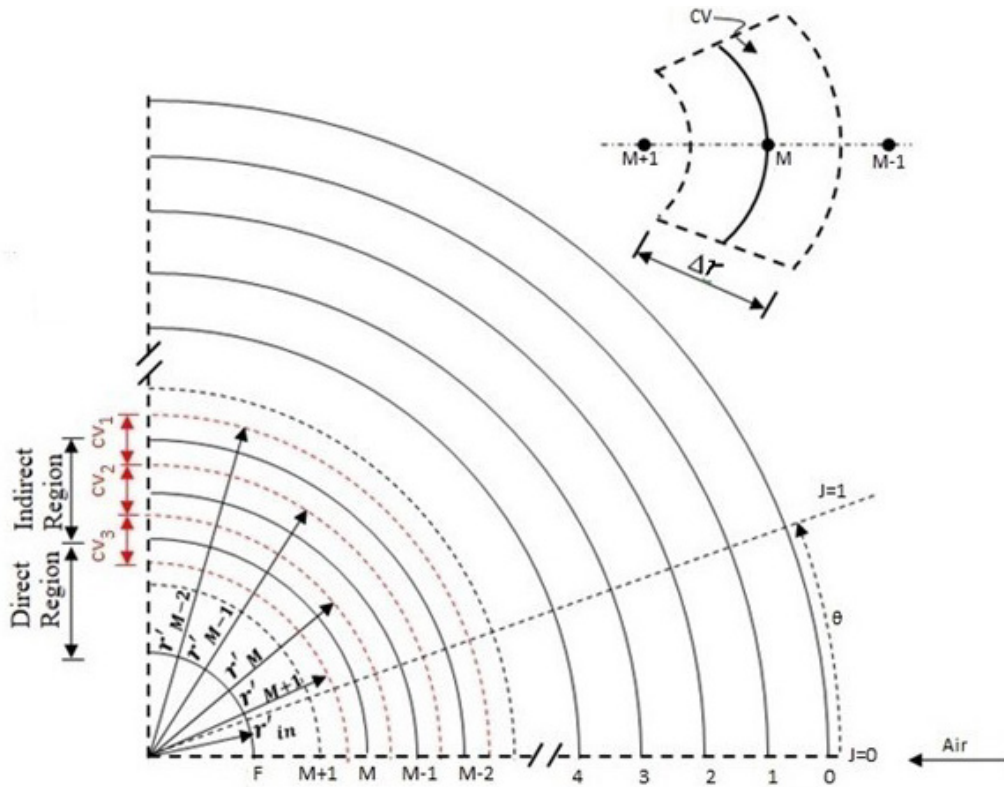


Fig. 2. Plan of Inverse analysis in a cylinder

Here, T_∞ is the ambient temperature and the temperature $T_1(t)$ as well as the heat flux $q_1(t)$ at a surface node are the unknown parameters. The unknowns $T_1(t)$ and $q_1(t)$ will be solved by the analysis of the energy balance approach among the control volumes.

1.2 Energy Balance Between Control Volumes

Consider (r_L, θ_J) as a one-dimensional line of analysis, where suffix J shows the azimuthal angle in terms of degrees of rotation in an anticlockwise direction, $J=0, 1, 2, \dots, J$. For the present case, consider (r_L, θ_0) as the line of analysis. The outer control surface of cv_1 is so assumed that the node $M-2$ lies at r_{out} . The connectivity between all the cv 's is so provided that the inner control surface of the preceding cv merges with the outer control surface of the succeeding cv . First, the energy balance is applied at cv_3 . To initiate the analysis, a prerequisite of known temperature-time history is needed at r_F and r_M . It provides the heat flux q_M to the inverse region, which subsequently determines temperatures at the nodes $M-1, M-2, \dots, 1$,

where node $M-2$ is the desired location of estimates at the surface.

To address circumferential issues, highly responsive thermocouples may be fixed below the outer surface at radius r_M of the metallic cylinder at different intervals along the azimuthal direction, which may be used for the measurement of transient temperature. Another method involves testing the cylinder with only two thermocouples fixed along the radial direction below the outer surface. In this method, the cylinder is rotated at different intervals along the azimuthal direction and transient temperature measurements are taken.

1.3 Heat Balance Equation

Heat accumulated within the

$$cv = (\text{Heat input to } cv) - (\text{Heat exit from } cv).$$

At node M :

$$\Delta r (r'_M + r'_{M+1}) \rho C \frac{\partial f_M}{\partial t} = \frac{2Kr'_{M+1}}{\Delta r} (T_{M+1} - f_M) + \frac{2Kr'_M}{\Delta r} (T_{M-1} - f_M), \quad (4)$$

At node $M-1$:

$$\Delta r(r'_{M-1} + r'_{M'})\rho C \frac{\partial T_{M-1}}{\partial t} = \frac{2Kr'_{M'}}{\Delta r}(f_M - T_{M-1}) + \frac{2Kr'_{M-1}}{\Delta r}(T_{M-2} - T_{M-1}), \quad (5)$$

At node $M-2$:

$$\Delta r(r'_{M-2} + r'_{M-1})\rho C \frac{\partial T_{M-2}}{\partial t} = \frac{2Kr'_{M-1}}{\Delta r}(T_{M-1} - T_{M-2}) + \frac{2Kr'_{M-2}}{\Delta r}(T_{M-3} - T_{M-2}). \quad (6)$$

Using Fourier's law of heat conduction and the boundary conditions for $t > 0$ at $r = r_M$ and at $r = r_{M-2}$, Eqs. (7) and (8) for temperature can be represented.

$$T_{M+1} = T_{M-1} + \frac{2q_M \Delta r}{K}, \quad (7)$$

$$T_{M-3} = T_{M-1} - \frac{2q_{M-2} \Delta r}{K}. \quad (8)$$

Hence, the modified form of the equation at node M on substitution of T_{M+1} is

$$T_{M-1} = f_M + \frac{1}{2} \frac{(\Delta r)^2}{\alpha} \frac{\partial f_M}{\partial t} - \frac{r'_{M+1}}{(r'_M + r'_{M+1})} \frac{2q_M (\Delta r)}{K}, \quad (9)$$

which in turn substituted in Eq. (10) at node $M-1$ that is modified as

$$T_{M-2} = f_M + \left(\frac{r'_{M-1} + r'_M}{r'_{M-1}} \right) \left[\frac{(\Delta r)^2}{\alpha} \frac{\partial f_M}{\partial t} + \frac{(\Delta r)^4}{4\alpha^2} \frac{\partial^2 f_M}{\partial t^2} - \left(\frac{r'_{M+1}}{r'_M + r'_{M+1}} \right) \frac{(\Delta r)^3}{K\alpha} \frac{\partial q_M}{\partial t} - \frac{2q_M (\Delta r) r'_{M+1}}{K(r'_M + r'_{M+1})} \right], \quad (10)$$

The substitution of T_{M-1} , T_{M-2} and T_{M-3} in the equation at node $M-2$ provides heat flux q_{M-2} at node $M-2$, which is expressed as

$$q_{M-2} = \frac{K\Delta r}{4r'_1\alpha} (r'_{M-2} + r'_{M-1}) \left[\frac{2\alpha f_M}{(\Delta r)^2} + \frac{\partial f_M}{\partial t} - \frac{4\alpha q_M}{K\Delta r} \frac{r'_{M+1}}{r'_M + r'_{M+1}} - \frac{2\alpha T_{M-2}}{(\Delta r)^2} - \frac{\partial T_{M-2}}{\partial t} \right]. \quad (11)$$

Finally, considering five nodes from the surface at $L=0, 1, 2, 3$ and 4 , as shown in Fig. 2, by considering node 1 at r_{out} (at $L=M-2=1$ if $r_{out}=r_1$), node M at r_M (at $L=M=3$ if $r_M=r_3$), node $M-1$ at r_{M-1} (at $L=M-1=2$ if $r_{M-1}=r_2$), node $M+1$ at r_{M+1} (at $L=M+1=4$ if $r_{M+1}=r_4$) and node 0 as fictitious node after node 1. The above

equations, which represent estimates of temperature and heat flux at node $L=M-2=1$, will be expressed as the surface node, which can be rewritten as follows:

$$T_1 = f_3 + \left(\frac{r'_2 + r'_3}{r'_2} \right) \left[\frac{(\Delta r)^2}{\alpha} \frac{\partial f_3}{\partial t} + \frac{(\Delta r)^4}{4\alpha^2} \frac{\partial^2 f_3}{\partial t^2} - \left(\frac{r'_4}{r'_3 + r'_4} \right) \frac{(\Delta r)^3}{K\alpha} \frac{\partial q_3}{\partial t} - \frac{2q_3 (\Delta r) r'_4}{K(r'_3 + r'_4)} \right], \quad (12)$$

$$q_1 = \frac{K\Delta r}{4r'_1\alpha} (r'_1 + r'_2) \left[\frac{2\alpha f_3}{(\Delta r)^2} + \frac{\partial f_3}{\partial t} - \frac{4\alpha q_3}{K\Delta r} \frac{r'_4}{r'_3 + r'_4} - \frac{2\alpha T_1}{(\Delta r)^2} - \frac{\partial T_1}{\partial t} \right]. \quad (13)$$

In a similar way, a heated flat plate of isotropic material having no internal heat generation, when subjected to an external flow of fluid of constant fluid properties, undergoes unsteady temperature variation at any point on its surface. Hence, a one-dimensional mathematical statement of the problem can be represented in cartesian coordinates by considering cylindrical coordinates within the limits of all radii tending to infinity. So, the equations for estimates of temperature and heat flux obtained in cylindrical coordinates can be modified, as shown below, assuming $r'_{(M-2)} = r'_{(M-1)} = r'_M = r'_{(M+1)} = r'$, for which Fig. 2 can be referred. The derivatives in the equations have been approximated by the finite difference approach.

$$T_{M-2} = f_M + 2 \frac{(\Delta r)^2}{\alpha} \frac{\partial f_M}{\partial t} + \frac{(\Delta r)^4}{2\alpha^2} \frac{\partial^2 f_M}{\partial t^2} - \frac{(\Delta r)^3}{K\alpha} \frac{\partial q_M}{\partial t} - \frac{2q_M (\Delta r)}{K}, \quad (14)$$

$$q_{M-2} = \frac{K}{\Delta r} (f_M - T_{M-2}) + \frac{K\Delta r}{2\alpha} \left[\frac{\partial f_M}{\partial t} - \frac{\partial T_{M-2}}{\partial t} \right] - q_M \quad (15)$$

2 EXPERIMENTAL APPROACH FOR VALIDATION

Validation of the derived equations was conducted using a hollow cylinder initially heated and a flat plate initially unheated. An experimental model of the cylinder shown in Fig. 3 was placed in a test section of the subsonic wind tunnel with dimensions of $0.3 \text{ m} \times 0.3 \text{ m}$ and 0.6 m long, as shown in Fig. 4. After initial heating of the hollow cylinder by means of

inbuilt heating element, it was allowed to cool under the flow of air at ambient condition. The model of a flat plate was kept in an insulated chamber, which was subjected to heating by means of a hot plate followed by intermittent blow of air.

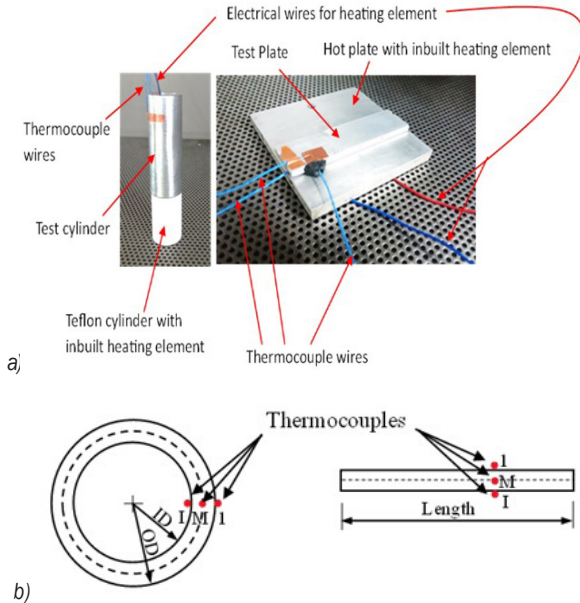


Fig. 3. Experimental models a) real experimental tool; b) a scheme

Both models were made of aluminium ($K=200$ W/(mK)), thermal diffusivity ($\alpha = 7.4 \times 10^{-5}$ m²/s) in which three T-type thermocouples of size 0.1 mm were

fixed in the material. Of the three thermocouples, two were placed at the in and out extreme surfaces while one was placed at the centre of the wall thickness along the line of surface normal. Hence, all three thermocouples lie in a straight line. The dimensions of the cylindrical model were $ID = 22$ mm, $OD = 31.6$ mm and height = 125 mm, and that of the flat plate model was length = 125 mm, width = 50 mm, and thickness = 5 mm.

The aluminium cylinder was fixed using a Teflon plug in the test section. A heating cartridge was pasted on one part of the plug, which fits into the aluminium cylinder. The other part of both the plugs was fitted into aluminium cylinders in such a way that the complete assembly is 0.3m in height. Thus, a high aspect ratio ($H/D = 9.49$) and a very low blockage ratio ($D/W = 0.105$) were obtained in the test section. Therefore, the dimension of the test cylinder is selected based on a high aspect ratio and very low blockage ratio, whereas the dimension of the plate is selected arbitrarily to suit available lab equipment.

As shown in Fig. 3, the surface with heat input is treated as F, which lies in the direct region, and the surface with heat exit is treated as I, which is in the inverse region, and an intermediate layer is considered at the centre of the wall thickness at M which is the interface of the direct and inverse region. At all these locations, the measurement of temperature vs time history was conducted; however, the thermocouple



Fig. 4. Experimental subsonic wind tunnel

at 1 has been used for the comparison with the temperature-time history obtained by the derived equation. NI PCIe6321 card with signal conditioner has been utilised for temperature acquisition, for which a LabVIEW program was written.

3 RESULTS AND DISCUSSION

3.1 Heated Hollow Metallic Cylinder Cooled in Crossflow of Air

Fig. 5 illustrates the time history of temperature measured at node 1, i.e., $T(1)$, when an initially heated cylinder was allowed to cool via air flowing in a subsonic wind tunnel.

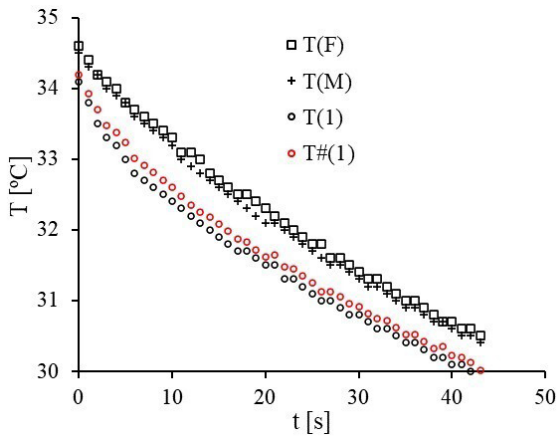


Fig. 5. Comparison of measured and estimated temperature vs time history for initially heated hollow cylinder placed in the flow of air

Simultaneously measured temperature histories at nodes F and M , i.e., $T(F)$ and $T(M)$, are also represented, which were utilised to estimate a simultaneous time history of temperature at node 1, i.e., T^*_1 (estimated surface temperature in $^{\circ}\text{C}$ by derived equation, i.e., T_1), which is obtained from derived Eq. (12) of temperature. The standard deviation σ of T^*_1 and $T(1)$ was then estimated and subtracted from the T^*_1 ; thereby, the estimated temperature-time history at node 1 as $T\#(1)$ has been illustrated in the figure.

Hence, the empirical form of temperature estimate at the surface can be represented as:

$$T\#(1) = T^*_1 - \sigma. \quad (16)$$

It is hereby made clear that the σ must be evaluated only once when the uncertainty has to be evaluated. Fig. 6 illustrates the percentage deviation between $T\#(1)$ and measured $T(1)$, which was

consequently found to be less than 0.5 %. The heat fluxes were then estimated using the derived Eq. (13) for the case of cylinder, which can be depicted in Fig. 7.

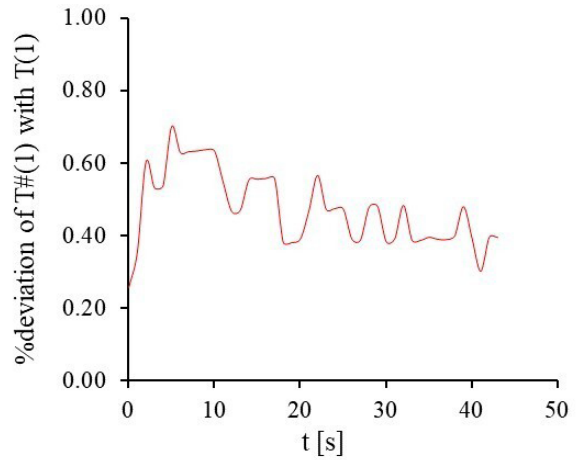


Fig. 6. Percentage deviation between measured temperature history $T(1)$ and estimated temperature history $T\#(1)$ for initially heated hollow cylinder placed in the flow of air

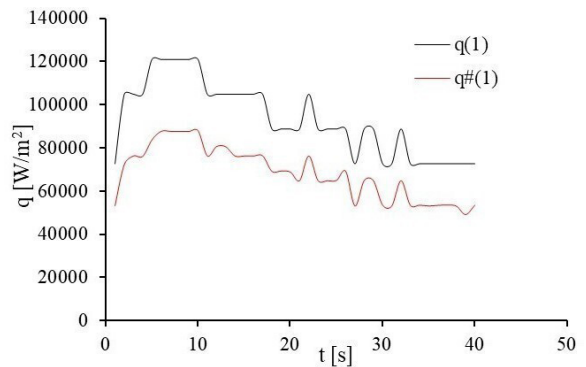


Fig. 7. Comparison of heat fluxes using derived equation by means of measured as well as estimated temperature - time history for initially heated hollow cylinder placed in the flow of air

The presented methodology explains that $T(F)$ is the temperature of the inner hot surface, which is ideally at an unchanged temperature. The wall material (metallic aluminium) will have extremely low temperature gradients. $T(1)$ is the temperature at the outer surface, which is treated as an interface of internal and surface resistances. This surface is always exposed to the flow of ambient air. As a result, the surface temperature drops drastically with the airflow and raises temperature gradients along the $F-M-1$ direction. The combined effect of inner hotness and outer cooling initially results in very low temperature gradients followed by gradually increasing temperature gradients along $F-M-1$. From

the experiments, a noticeable temperature gradient was observed approximately at the middle plane, which was why the M was taken as the centre of $F-1$. Hence, the $T(F)$ and $T(M)$ have a small difference, while $T(M)$ and $T(1)$ have a large difference. It illustrates the heat fluxes estimated using temperature estimates $T\#(1)$ obtained from Eq. (16) represented by $q\#(1)$ and measured temperatures $T(1)$ represented by $q(1)$. The estimated heat flux $q\#(1)$ shows reasonably good consistency with heat flux $q(1)$; however, the consistent deviation between them is due to the temperature estimate's deviation between $T\#(1)$ and $T(1)$ as of approximation errors that will always exist because $T\#(1)$ is estimates and not the exact.

3.2 A Heated Flat Plate in Still Air

Fig. 8 illustrates the time history of temperature measured at node 1, i.e., $T(1)$, simultaneous measured temperature histories at nodes F and M , i.e., $T(F)$ and $T(M)$, which were utilised to estimate a simultaneous time history of temperature at node 1, i.e., T^*_1 and subsequently $T\#(1)$ using Eqs. (14) and (16), respectively, when one surface of a flat plate was heated with a consistent heating source, and the other surface was exposed to an ambient environment of atmospheric condition.

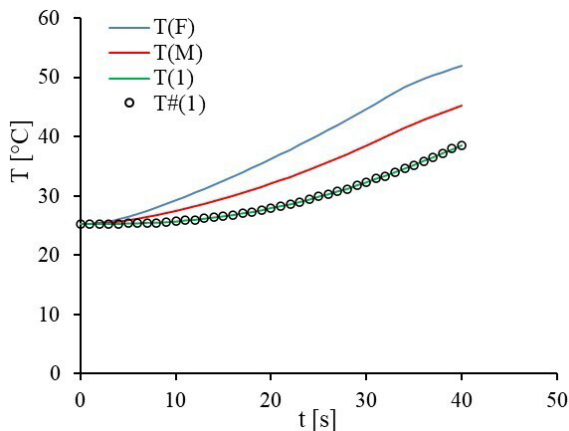


Fig. 8. Comparison of measured and estimated temperature vs time history for flat plate heated in an ambient environment of atmospheric condition

The percentage deviation of $T\#(1)$ with measured $T(1)$ was consequently found to be less than 0.03 %, as shown in Fig. 9.

Fig. 10 illustrates the comparative variations between estimated surface heat flux obtained by using the derived Eq. (15) considering temperature estimates $T\#(1)$ of Fig. 8 represented by $q\#(1)$ and by

considering measured temperatures $T(1)$ represented by $q(1)$. Both exhibit remarkably good consistency with negligible deviations.

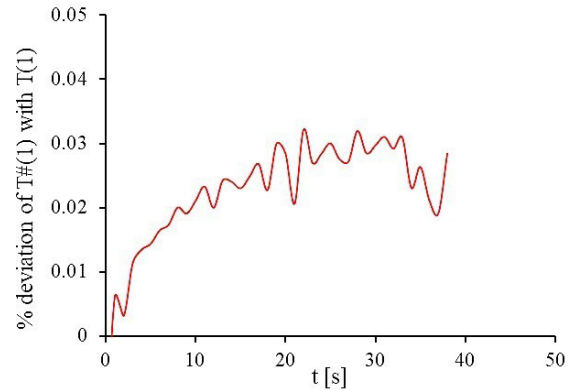


Fig. 9. Percentage deviation between measured temperature history $T(1)$ and estimated temperature history $T\#(1)$ for flat plate heated in an ambient environment of atmospheric condition

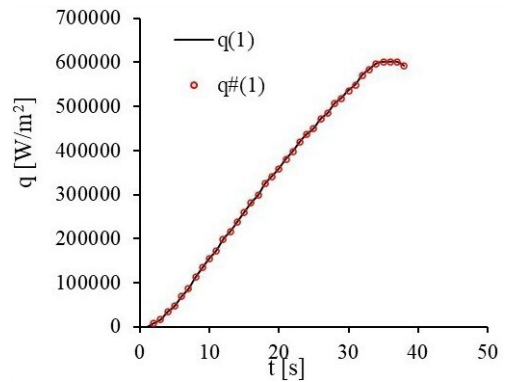


Fig. 10. Comparison of heat fluxes using derived equation by means of measured as well as estimated temperature vs time history for flat plate heated in an ambient environment of atmospheric condition

3.3 A Heated Flat Plate when Cooled in Still Air with Random Air Blows

Fig. 11 illustrates the time history of temperature measured at node 1, i.e., $T(1)$, simultaneous measured temperature histories at nodes F and M , i.e., $T(F)$ and $T(M)$, which were utilised to estimate a simultaneous time history of temperature at node 1, i.e. T^*_1 and subsequently $T\#(1)$ using Eqs. (14) and (16), respectively, when one surface of a flat plate was heated with a consistent heating source, and the other surface was exposed to an ambient environment of atmospheric condition, which was given random air blow at 35 °C. Simultaneously measured temperature histories at nodes F and M , i.e., $T(F)$ and $T(M)$, are also represented, which were utilized to estimate a

corresponding time history of temperature at node 1, i.e. T^*_1 , by means of presented derived Eq. (14) of temperature.

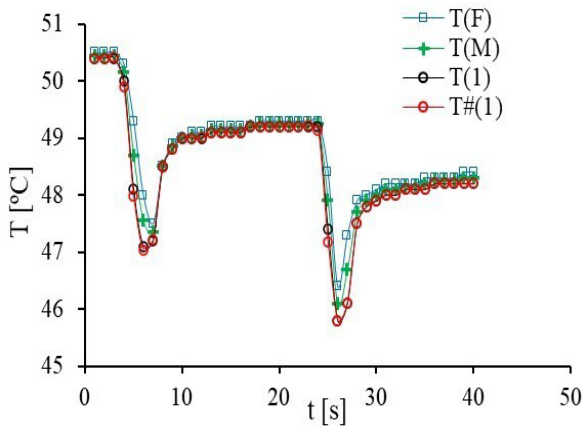


Fig. 11. Comparison of measured and estimated temperature vs time history for initially heated flat plate given random air blows

The percentage deviation of $T\#(1)$ with measured $T(1)$ was consequently found for the initially heated flat plate given with random air blows, showing less than 0.01 % when no blow was given and it is less than 0.5 % when a blow was given, which can be depicted respectively in Figs. 12 13, showing the comparative variations between heat fluxes obtained by using derived Eq. (15) considering $T\#(1)$ and $T(1)$ i.e., by means of estimated as well as measured temperature vs time history, respectively, for the initially heated flat plate given random air blows. $q\#(1)$ exhibits remarkably good consistency with $q(1)$ with negligible deviations.

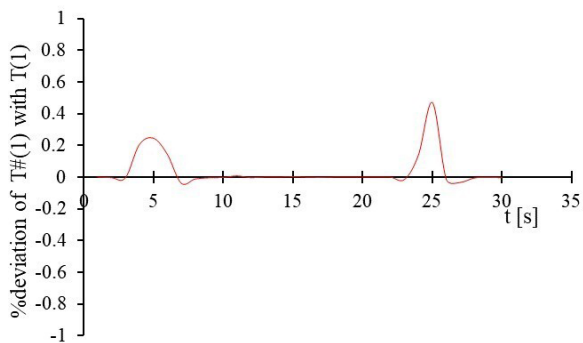


Fig. 12. Percentage deviation between measured temperature history $T(1)$ and estimated temperature history $T\#(1)$ for initially heated flat plate given random air blows

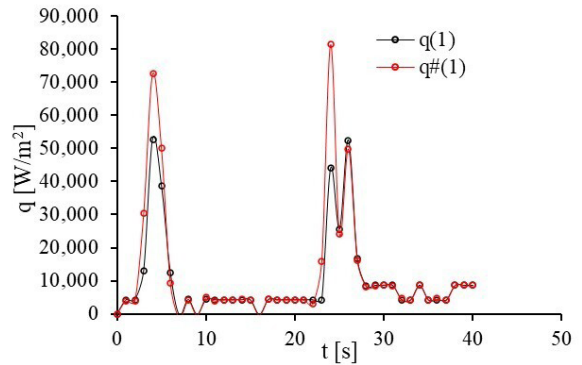


Fig. 13. Comparison of heat fluxes using derived equation by means of measured as well as estimated temperature vs time history for initially heated flat plate given random air blows

4 VALIDATIONS WITH THE EARLIER PUBLISHED LITERATURE

A comparison of derived equations in the present study was conducted with the reported literature by Burggraaf [40] for both estimated temperature and heat flux at the surface, which can be observed in Figs. 14 to 16. Burggraaf [40] has given an exact solution for IHCP in various geometrical shapes. For the plane slab, the equation for the estimated temperature at the surface is expressed as:

$$T(x,t) = \left\{ T_0(t) + \sum_{n=1}^{\infty} \frac{1}{(2n)!} \left(\frac{x^2}{\alpha} \right)^n \frac{\partial^n T_0}{\partial t^n} \right\} - \frac{x}{K} \left\{ q_0(t) + \sum_{n=1}^{\infty} \frac{1}{(2n+1)!} \left(\frac{x^2}{\alpha} \right)^n \frac{\partial^n q_0}{\partial t^n} \right\}, \quad (17)$$

where x , $T(x,t)$, $T_0(t)$ and $q_0(t)$ represent respectively the thickness of the inverse region, the estimated temperature of the outer surface, the measured temperature at some inner location and the heat flux at the measured location. For $n = 2$, i.e., considering the first two terms of summation terms, the equation is represented as:

$$T(x,t) = \left\{ T_0(t) + \frac{1}{2} \frac{x^2}{\alpha} \frac{\partial T_0}{\partial t} + \frac{1}{24} \frac{x^4}{\alpha^2} \frac{\partial^2 T_0}{\partial t^2} \right\} - \frac{x}{K} \left\{ q_0(t) + \frac{1}{6} \frac{x^2}{\alpha} \frac{\partial q_0}{\partial t} + \frac{1}{120} \frac{x^4}{\alpha^2} \frac{\partial^2 q_0}{\partial t^2} \right\}, \quad (18)$$

Fig. 14 shows a comparison of estimated temperatures using derived Eq. (14) by means of measured temperature-time history between the present study and Burggraaf [40] for an initially heated flat plate given random air blows. The comparison

depicts consistent and close approximations throughout the time history.

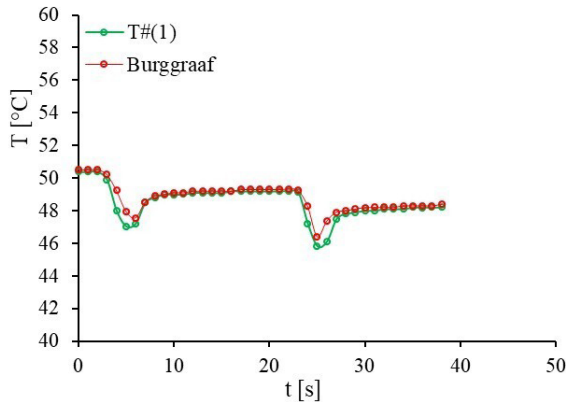


Fig. 14. Comparison of estimated temperatures using derived equation between the present study and Burggraaf for initially heated flat plate given random air blows

The heat flux equation reported by Burggraaf [40] is also shown by Eq. (19) and for $n = 2$, i.e., considering the first two terms of summation terms, the equation is represented by Eq. (20), where $q_s(t)$ is the estimated heat flux at the outer surface. The estimated heat flux in the present study was compared with Burggraaf [40] using the same measured temperatures in both equations.

$$q_\delta(t) = -\rho c \delta \sum_{n=1}^{\infty} \frac{1}{(2n-1)!} \left(\frac{\delta^2}{\alpha}\right)^{n-1} \frac{\partial^n T_0}{\partial t^n} + \bar{q}_0(t) + \sum_{n=1}^{\infty} \frac{1}{(2n)!} \left(\frac{\delta^2}{\alpha}\right)^{n-1} \frac{\partial^n q_0}{\partial t^n}, \quad (19)$$

$$q_s(t) = q_0(t) - \rho c x \frac{\partial T_0}{\partial t} - \rho c x \frac{1}{6} \frac{x^2}{\alpha} \frac{\partial^2 T_0}{\partial t^2} + \frac{1}{2} \frac{x^2}{\alpha} \frac{\partial q_0}{\partial t} + \frac{1}{24} \frac{x^4}{\alpha^2} \frac{\partial^2 q_0}{\partial t^2}. \quad (20)$$

Comparisons of heat fluxes at the outer surface using derived Eq. (15) in the present study by means of measured as well as estimated temperature vs time history with Burggraaf [40] for the flat plate heated in an ambient environment of atmospheric condition shown in Fig. 15 as well as for initially heated flat plate given random air blows shown in Fig. 16. Both figures show reasonably good and consistent data of heat flux with the time history and establishes a favourable validation.

In Fig. 15, the difference between the results of the present study and the Burggraaf [40] results have increased over time as the third derivative of the

measured temperature f_M only in the present developed solution Eq. (15), which is apparent from simultaneous observation of Eqs. (14), (15) and (20). In Eq. (14), the second derivative of f_M exists, and further putting T_{M-2} from Eq. (14) in Eq. (15), there is an increase in the derivative of f_M from the second derivative to the third derivative due to the differentiation of term T_{M-2} . The presence of the third derivative term in Eq. (15) more accurately estimates the surface heat flux with time.

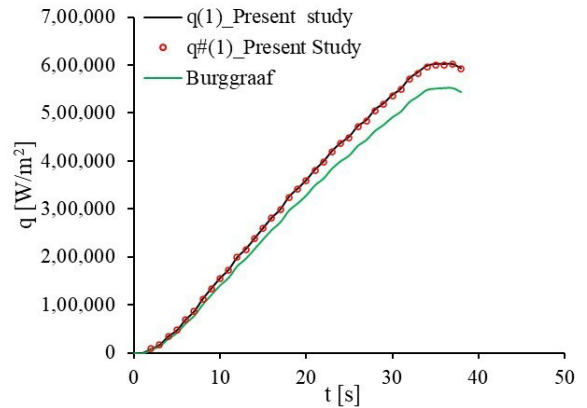


Fig. 15. Comparison of heat fluxes at the outer surface using the derived equation in the present study with Burggraaf for flat plate heated in an ambient environment of atmospheric condition

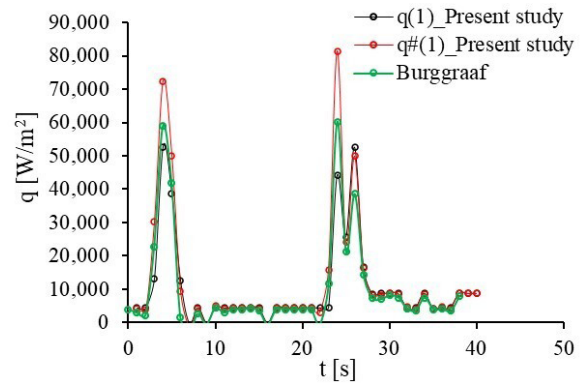


Fig. 16. Comparison of heat fluxes at the outer surface using the derived equation in the present study with Burggraaf for initially heated flat plate given random air blows

5 CIRCUMFERENTIAL DISTRIBUTION OF NUSSELT NUMBER IN A CYLINDER

An experiment was conducted to determine the circumferential distribution of the Nusselt number around the cylinder. The cylinder was a three-piece model assembled as a single cylinder. Of the three, two were Teflon cylinders of 22 mm ID, 31.9 mm OD and 135 mm height, while the test cylinder is of

copper having the same *ID* and *OD* as that of Teflon cylinders while the height was kept 30 mm. The copper test cylinder was fixed between the two Teflon cylinders so as to restrict the longitudinal flow of heat. Hence, variation of temperature takes place in radial and azimuthal (circumferential) direction only. The experimental setup and the cylinder in the wind tunnel test section (size: 0.3 m × 0.3 m × 0.6 m) have been shown in Fig. 4) while the original photographs and the schematic diagram of the test cylinder model have been shown in Fig. 17. The cartridge heating was done with a DC power supply. The cylinder was heated to 20 °C above the ambient temperature. For every reading at a 10° interval in the azimuthal direction from the front stagnation point, the cylinder was rotated by 10°. The Nusselt number (*Nu*) distribution thus obtained is represented in Fig. 18. The flow Reynolds number based on the diameter was kept at 35,000. The obtained *Nu* distribution was compared with the *Nu* distribution of Tsutsui and Igarashi [41], who conducted the experiments at Reynolds numbers of 31,000 and 41,000, as shown in Fig. 19. The *Nu* distribution obtained from the present methodology was well in agreement with those of Tsutsui and Igarashi [41].

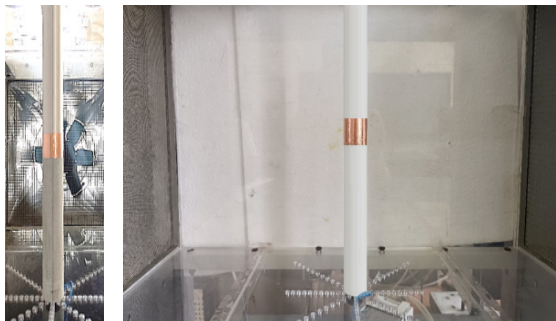


Fig. 17. Photographs of a cylinder in the test section of the wind tunnel

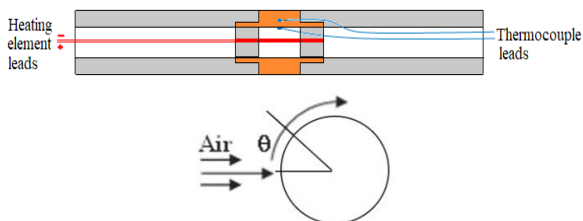


Fig. 18. Schematic diagram of the cylinder assembly

6 CONCLUSIONS

A novel approach developed to estimate the surface temperature and surface heat flux has been explained

in the present paper. The approach is based on the inverse heat conduction method, where the heat flow domain is divided into some control volumes, and the energy balance between them is analysed to arrive at equations for temperature and heat flux estimations. The derived equations were tested by conducting experiments that show very close approximations with respect to the exact data. All the estimates lie within 0.5 % deviations from the exact data, which is very close data; however, the flat plate smooth cooling or heating shows extremely close data within 0.03 %. To address the circumferential variation of the heat transfer, an experimental approach of validation was conducted in a wind tunnel for a crossflow of air with a cylinder under constant heat flux conditions that validates well with the reported literature data. Hence, the proposed methodology of the inverse heat conduction approach is valid and recommended to be used.

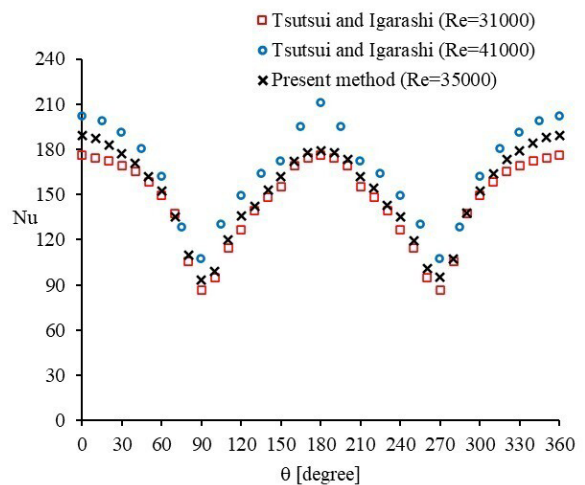


Fig. 19. Nusselt number distribution over a single cylinder obtained from the present methodology and its comparison with the *Nu* distribution of Tsutsui and Igarashi [41]

7 ACKNOWLEDGEMENTS

The authors express their gratitude for the facility provided by the Department of Mechanical Engineering, B.I.T. Mesra, Ranchi, India.

8 NOMENCLATURES

<i>C</i>	specific heat, [J/kg°C]
<i>cv</i>	control volume,
<i>f_M</i>	measured transient temperature at node 3, [°C]
<i>h(t)</i>	heat transfer coefficient, [W/(m²K)]

k	thermal conductivity, [W/(m°C)]
ρ	density, [kg/m ³]
$q_M(t)$	calculated heat flux at sensor location on time t , [W/m ²]
$q_M^*(t)$	estimated surface heat flux at time t , [W/m ²]
r	radius, [m]
Δr	thickness of each control volume,
T_∞	measured ambient temperature, [°C]
T^*_1	estimated surface temperature by derived equation, [°C]
T_1	measured real time surface transient temperature, [°C]
$T^{\#}_1$	estimated surface temperature, [°C]

9 REFERENCES

- [1] Taler, J. (2007). Determination of local heat transfer coefficient from the solution of the inverse heat conduction problem. *Forsch Ingenieurwes*, vol. 71, p. 69-78, DOI:10.1007/s10010-006-0044-2.
- [2] Golsorkhi, N.A., Tehrani, H.A. (2014). Levenberg-marquardt method for solving the inverse heat transfer problems. *Journal of Mathematics and Computer Science*, vol. 13, no. 4, p. 300-310, DOI:10.22436/jmcs.013.04.03.
- [3] Cuadrado, D.G., Marconnet, A., Paniagua, G. (2020). Non-Linear non-iterative transient inverse conjugate heat transfer method applied to microelectronics. *International Journal of Heat and Mass Transfer*, vol. 152, 119503, DOI:10.1016/j.ijheatmasstransfer.2020.119503.
- [4] Bohacek, J., Kominek, J., Vakharushev, A., Karimi-Sibaki, E., Lee, T.W. (2021). A sequential inverse heat conduction problem in OpenFOAM. *Open Foam® Journal*, vol. 1, p. 27-46, DOI:10.51560/ofj.v1.33.
- [5] Felde, I., Reti, T. (2010). Evaluation of hardening performance of cooling media by using inverse heat conduction methods and property prediction. *Strojniški vestnik - Journal of Mechanical Engineering*, vol. 56, no. 2, p. 77-83.
- [6] Charifi, M., Zegadi, R. (2017). Inverse Method for controlling pure material solidification in spherical geometry. *Strojniški vestnik - Journal of Mechanical Engineering*, vol. 63, no. 2, p. 103-110, DOI:10.5545/sv-jme.2016.3805.
- [7] Gostimirović, M., Sekulić, M., Kopač, J., Kovač, P. (2011). Optimal control of workpiece thermal state in creep-feed grinding using Inverse heat conduction analysis. *Strojniški vestnik - Journal of Mechanical Engineering*, vol. 57, no. 10, p. 730-738, DOI:10.5545/sv-jme.2010.075.
- [8] Hriberšek, M., Šajin, V., Pušavec, F., Rech, J., Kopač, J. (2016). The procedure of solving the inverse problem for determining surface heat transfer coefficient between liquefied nitrogen and inconel 718 workpiece in cryogenic machining. *Strojniški vestnik - Journal of Mechanical Engineering*, vol. 62, no. 6, p. 331-339, DOI:10.5545/sv-jme.2016.3572.
- [9] Stolz, G. (1960). Numerical solutions to an inverse problem of heat conduction for simple shapes. *Journal of Heat Transfer*, vol. 82, no. 1, p. 20-25, DOI:10.1115/1.3679871.
- [10] Frank, I. (1963). An application of least squares method to the solution of the inverse problem of heat conduction. *Journal of Heat Transfer*, vol. 85, no. 4, p. 378-379, DOI:10.1115/1.3686128.
- [11] Sparrow, E.M., Sheikh, A.H., Lundgren, T.S. (1964). The inverse problem in transient heat conduction. *Journal of Applied Mechanics*, vol. 31, no. 3, p. 369-375, DOI:10.1115/1.3629649.
- [12] Beck, J.V., Wolf, H. (1965). The nonlinear inverse heat conduction problem. *ASME, Paper No. 65-HT-40*.
- [13] Beck, J.V. (1970). Nonlinear estimation applied to the nonlinear heat conduction. *International Journal of Heat and Mass Transfer*, vol. 13, no. 4, p. 703-716, DOI:10.1016/0017-9310(70)90044-X.
- [14] Imber, M., Khan, J. (1972). Prediction of transient temperature distributions with embedded thermocouples. *AIAA Journal*, vol. 10, no. 6, p. 784-789, DOI:10.2514/3.50211.
- [15] Weber, C.F. (1981). Analysis and solution of the ill-posed inverse heat conduction problem. *International Journal of Heat and Mass Transfer*, vol. 24, no. 11, p. 1783-1792, DOI:10.1016/0017-9310(81)90144-7.
- [16] Raynaud, M., Beck, J.V. (1988). Methodology for comparison of inverse heat conduction methods. *ASME Journal of Heat and Mass Transfer*, vol. 110, no. 1, p. 30-37, DOI:10.1115/1.3250468.
- [17] Li, H.Y., Yan, W.M. (1999). Estimation of wall heat flux in an inverse convection problem. *Journal of Thermophysics and Heat Transfer*, vol. 13, no. 3, p. 394-396, DOI:10.2514/2.6456.
- [18] Masanori, M., Hirofumi, A., Yuhichi, M. (2003). Estimation of surface temperature and heat flux using inverse solution for one-dimensional heat conduction. *ASME Journal of Heat and Mass Transfer*, vol. 125, no. 2, p. 213-223, DOI:10.1115/1.1560147.
- [19] Chen, C.K., Wu, L.W., Yang, Y.T. (2005). Estimation of unknown outer-wall heat flux in turbulent circular pipe flow with conduction in the pipe wall. *International Journal of Heat and Mass Transfer*, vol. 48, no. 19-20, p. 3971-3981, DOI:10.1016/j.ijheatmasstransfer.2005.04.022.
- [20] Jang, H.Y., Tuan, P.C., Chen, T.C., Chen, T.S. (2006). Input estimation method combined with the finite-element scheme to solve IHCP hollow-cylinder inverse heat conduction problems. *Numerical Heat Transfer, Part A: Applications: An International Journal of Computation and Methodology*, vol. 50, no. 3, p. 263-280, DOI:10.1080/10407780600602473.
- [21] Chen, C.K., Wu, L.W., Yang, Y.T. (2006). Application of the inverse method for the estimation of heat flux and temperature on the external surface in laminar pipe flow. *Applied Thermal Engineering*, vol. 26, no. 14-15, p. 1714-1724, DOI:10.1016/j.applthermaleng.2005.11.006.
- [22] Wikstrom, P., Blasiak, W., Berntsson, F. (2007). Estimation of the transient surface temperature and heat flux of a steel slab using an inverse method. *Applied Thermal Engineering*, vol. 27, no. 14-15, p. 2463-2472, DOI:10.1016/j.applthermaleng.2007.02.005.
- [23] Dennis, B.H., Dulikravich, S.G.S. (2012). Inverse determination of unsteady temperatures and heat fluxes on inaccessible boundaries. *Journal of Inverse and Ill-Posed Problem*, vol. 20, p. 791-803, DOI:10.1515/jip-2012-0052.
- [24] Kim, S.K., Lee, W. (2002). Solution of inverse heat conduction problems using maximum entropy method. *International*

- Journal of Heat and Mass Transfer*, vol. 45, no. 2, p. 381-391, DOI:10.1016/S0017-9310(01)00155-7.
- [25] Cebula, A., Taler, J. (2014). Determination of transient temperature and heat flux on the surface of a reactor control rod based on temperature measurements at the interior points. *Applied Thermal Engineering*, vol. 63, no. 1, p. 158-169, DOI:10.1016/j.applthermaleng.2013.10.066.
- [26] Dhiman, S.K., Prasad, J.K. (2017). Inverse estimation of heat flux from a hollow cylinder in crossflow of air. *Applied Thermal Engineering*, vol. 113, p. 952-961, DOI:10.1016/j.applthermaleng.2016.11.088.
- [27] Singh, S.K., Yadav, M.K., Sonawane, R., Khandekar, S., Muralidhar, K. (2017). Estimation of time-dependent wall heat flux from single thermocouple data. *International Journal of Thermal Sciences*, vol. 115, p. 1-15, DOI:10.1016/j.ijthermalsci.2017.01.010.
- [28] Cebula, A., Taler, J., Ochoń, P. (2018). Heat flux and temperature determination in a cylindrical element with the use of finite volume finite element method. *International Journal of Thermal Sciences*, vol. 127, p. 142-157, DOI:10.1016/j.ijthermalsci.2018.01.022.
- [29] Duda, P., Konieczny, M. (2019). A new algorithm for solving an inverse transient heat conduction problem by dividing a complex domain into parts. *International Journal of Heat and Mass Transfer*, vol. 128, p. 865-874, DOI:10.1016/j.ijheatmasstransfer.2018.09.064.
- [30] Mehta, R.C. (2020). *Influence of Input Parameters on the Solution of Inverse Heat Conduction Problem*, Intech Open, London, DOI:10.5772/intechopen.91000.
- [31] Da Silva, W.B., Dutra, J.C.S., Kopperschmidt, C.E.P., Lesnic, D., Aykroyd, R.G. (2021). Sequential particle filter estimation of a time-dependent heat transfer coefficient in a multidimensional nonlinear inverse heat conduction problem. *Applied Mathematical Modelling*, vol. 89, p. 654-668, DOI:10.1016/j.apm.2020.07.020.
- [32] Shahnazari, M.R., Shali, F.R., Saberi, A., Moosavi, M.H. (2021). A new hybrid method for solving inverse heat conduction problems. *International Journal of Mechanics*, vol. 15, p. 151-158, DOI:10.46300/9104.2021.15.17.
- [33] Matsevityi, Y.M., Strel'nikova, E.A., Povgorodnii, V.O., Safonov, N.A., Ganchin, V.V. (2021). Methodology of solving inverse heat conduction and thermo elasticity problems for identification of thermal processes. *Journal of Engineering Physics and Thermophysics*, vol. 94, p. 1110-1116, DOI:10.1007/s10891-021-02391-w.
- [34] Seryakov, A. (2022). The solving of the inverse thermal conductivity problem for study the short linear heat pipes. *Engineering*, vol. 14, p. 185-216, DOI:10.4236/eng.2022.146018.
- [35] Gomez, C.F., Nieuwenhuizen, R., van der Geld, C.W.M., Kuerten, H.G.M., Bsibsi, M., van Esch, B.P.M. (2022). Inaccuracies in the inverse heat conduction problem solution and their effect on the estimation of heat fluxes during quenching. *International Journal of Heat and Mass Transfer*, vol. 194, 122953, DOI:10.1016/j.ijheatmasstransfer.2022.122953.
- [36] Leu, J.S., Tu, T.W. (2022). An effective analytical method in inverse heat transfer conduction problem with measured temperature time history at remote boundary. *Heat Transfer Research*, vol. 53, no. 7, p. 19-38, DOI:10.1615/HeatTransRes.2022039767.
- [37] Ciałkowski, M., Olejnik, V., Joachimiak, M., Grysa, K., Frąckowiak, A. (2022). Cauchy type nonlinear inverse problem in a two-layer area. *International Journal of Numerical Methods for Heat & Fluid Flow*, vol. 32, no.1, p. 313-331, DOI:10.1108/HFF-09-2020-0584.
- [38] Roy, A.D., Dhiman, S.K. (2023). Solutions of one-dimensional inverse heat conduction problems: a review. *Transactions of the Canadian Society for Mechanical Engineering*, vol. 47, no. 3, p. 271-285, DOI:10.1139/tcsme-2022-0157.
- [39] Holman, J.P. (1990). *Heat Transfer*, 10th ed. McGraw-Hill, New York.
- [40] Burggraaf, O.R. (1964). An exact solution of the inverse problem in heat conduction theory and applications. *ASME Journal of Heat Transfer*, vol. 86, no. 3, p. 373-382, DOI:10.1115/1.3688700.
- [41] Tsutsui, T., Igarashi, T. (2006). Heat transfer enhancement of a circular cylinder. *ASME Journal of Heat and Mass Transfer*, vol. 128, no. 3, p. 226-233, DOI:10.1115/1.2150832.